On the Isomerism of [1$_n$]Ketonand and [1$_n$]Starand

Sungu Hwang, Gean Ha Ryu,† Yun Hee Jang,‡ and Doo Soo Chung*

Department of Chemistry, Seoul National University, Seoul 151-742, Korea
Received June 30, 1999

Ionophores have been extensively investigated due to their possible application for such diverse processes as isotope separation, ion transport through membrane, and transport of therapeutic doses of radiation to tumor sites.[1] New classes of supramolecular ionophore, [1$_n$]orthocyclophanepolyones ([1$_n$]ketonands) and |1$_n$|orthocyclophane-2n-crown-n ([1$_n$]-starands), were recently synthesized and characterized by Lee *et al.*[2-7] The ionophores were obtained from the oxidation of |1$_n$|orthocyclophane ([1$_n$]OCP). In general, the oxidation of the even-numbered [1$_n$]OCPdiones (n = 6 and 8) results in |1$_n$|starands, while the oxidation of the odd-numbered |1$_n$|OCPdiones (n = 5 and 7) results in |1$_n$|ketonands. However, oxidation of |1$_4$|OCPdione with ceric ammonium nitrate (CAN) gave |1$_4$|OCPtetraone ([1$_4$]ketonand) in 61% yield, instead of the expected |1$_4$|starand.[8]

In this work, we carried out semi-empirical MNDO calculations on the |1$_n$|ketonands (**1, 2, 3, 4**) and [1$_n$]starands (**5, 6, 7, 8**), and free energy perturbation (FEP) simulations on the isomerization between ketonand and starand in order to rationalize the experimental findings and understand the isomerism between |1$_n$|ketonand and [1$_n$]starand. The energy calculation on **1**, **3**, **5** and **7** had been attempted by Cho, *et al.* who had performed an *ab initio* study on the model compounds in which the phenyl rings of |1$_n$|OCPs were replaced by simpler C–C bonds.[9] They explained the stability of |1$_4$|ketonand and [1$_6$|starand in terms of building-unit energy, Coulombic energy, and non-Coulombic strain energy. However, their work is limited to even-numbered |1$_n$|starands and [1$_n$]ketonands. In this work, we performed the theoretical studies on the full series of |1$_n$|starands and [1$_n$]ketonands from n = 4 to 7 without any simplification of the structures.

Computational Details

In the present work, we carried out semi-empirical quantum-mechanical MNDO[10] calculations implemented in the GAMESS package[11] on the full compounds **1-8**, shown in Figure 1, without any simplification. The geometry was fully optimized in a C_1 symmetry (that is, without any symmetry restriction) by using the quasi-Newton-Raphson

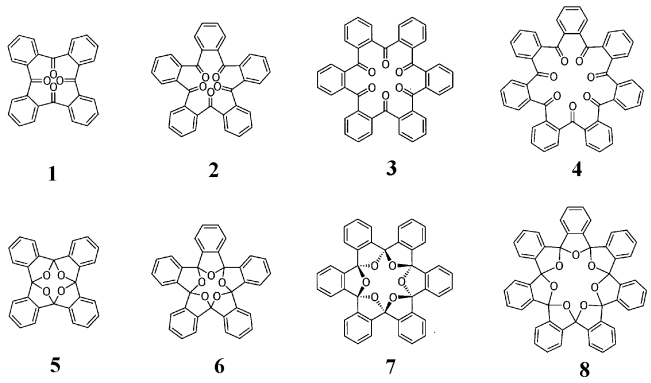

Figure 1. The chemical structures of [1$_n$]ketonand and [1$_n$]starand (n = 4–7).

procedure[12] until the root-mean-square gradient less than 3.3×10^{-6} hartree/bohr (= 0.0036 kcal/mol/Å) was reached.

In addition, the entropy change from |1$_n$|ketonand to |1$_n$|starand was estimated by performing the MNDO calculations and the free energy perturbation (FEP) calculations.[13] In FEP calculation, a mutation from one state (A) to the other (B) is done by using a coupling parameter λ to smoothly convert the potential V of A (λ = 0) into that of B (λ = 1). A hypothetical intermediate potential V_λ is defined as $V_\lambda = (1-\lambda)V_1 + \lambda V_2$ ($0 \le \lambda \le 1$). The free energy change (ΔG or ΔA) is calculated using the finite difference thermodynamic integration (FDTI) algorithm of Mezei.[14] The molecular dynamics (MD) simulation is used to generate the canonical ensembles from which a phase space is sampled for the integration. The FEP method allows the calculation of the free energy difference (ΔA) between two similar structures having the same types of chemical bonds by slowly perturbing one structure into the other.[15,16] For two systems having different types of bonds, however, only the contribution of the entropy ($-T\Delta S = \Delta A - \Delta E$) can be obtained from FEP calculations, since the force field used in the molecular mechanics (MM) and FEP calculations does not contain the information about the absolute value of bond dissociation energy. The FEP calculation was carried out using the CVFF force field implemented in *Discover* 95.0 molecular dynamics simulation package.[17] 240 dynamic windows were used with the equilibration for 20 ps and the data collection for 20 ps at each window. The entire simulation was performed with a time step of 1.0 fs at 300 K in vacuum. The energy difference ΔE between the two isomers was calculated by MM calculations with the same CVFF force field as used in the FEP calculation.

*Author to whom correspondence should be addressed. e-mail: dschung@snu.ac.kr. phone: +82-2-880-8130, Fax: +82-2-877-3025
†Present Address: Natural Science Research Institute, Jeonju University, Jeonju 560-759, Korea
‡Present Address: Materials and Process Simulation Center, Beckman Institute (139-74), California Institute of Technology, Pasadena, CA 91125, USA

Results and Discussion

At each MNDO optimized geometry, all the vibrational frequencies were calculated to be real, indicating that the obtained structure corresponds to a true minimum, not a saddle point. The root-mean-square (RMS) deviation of the structure from the x-ray crystallographic one (or from the previous work) is tabulated in Table 1. The optimized structure of |1$_6$|starand **7** in almost perfect agreement with the crystal structure.[4] and those of |1$_5$|ketonand **2** and |1$_7$|ketonand **4** are in modest agreement with the crystal structures.[6] The optimized structures of |1$_4$|starand **5** and |1$_6$|starand **7** are also in almost perfect agreement with those obtained by Cho. *et al.*[9]

The energy differences between |1$_n$|ketonand and |1$_n$|-starand are listed in Table 2. The comparison of the energies of the two optimized structures shows that ketonand is more stable than starand in the cases of |1$_4$| and |1$_5$|, while starand is more stable in the cases of |1$_6$| and |1$_7$|. Except for |1$_7$|, the calculation result is in good agreement with the experimental observations. The inclusion of the contribution from entropy can fix the discrepancy between theoretical and experimental results. Entropy was estimated with the rigid rotor–harmonic oscillator approximation. The vibrational frequencies were weighted by 0.89. The values of the $-T\Delta S$ and ΔA are also listed in Table 2. Calculated ΔA's are in good agreement with the experiments for all sizes of the ring. Since MNDO parameters are optimized to reproduce heats of formation, geometrical variables, dipole moments, and first vertical ionization potentials[10] rather than vibrational frequencies, the entropy estimated from MNDO may not be accurate. Thus we evaluate the entropy by the FEP simulation method.

Table 1. RMS deviation of the optimized structures from the crystal structures and those of previously reported theoretical work (MP2//HF/6-31G*)[9]

	RMS deviation (Å)	
	from crystal structure	from reference 9
[1$_4$]ketonand (**1**)	–	0.73
|1$_5$|ketonand (**2**)	0.32	–
|1$_6$|ketonand (**3**)	–	0.60
|1-|ketonand (**4**)	0.39	–
[1$_4$]starand (**5**)	–	0.08
[1$_6$]starand (**7**)	0.10	0.09

Table 2. The difference of thermodynamic quantities between [1$_n$]ketonand and |1$_n$|starand from MNDO calculations (|1$_n$|ketonand → [1$_n$]starand) (unit: kcal/mol)

Ring Size (n, |1$_n$|)	ΔE^a (MNDO)	$T\Delta S^b$ (MNDO)	ΔA^c (MNDO)
4	76.8	6.5	83.3
5	85.5	8.3	93.8
6	−23.9	11.7	−12.2
7	−4.7	12.1	7.4

[a]Energy difference Energy (|1$_n$|starand) – Energy (|1$_n$|ketonand). The positive value means that ketonand is more stable than starand. [b]The entropy is estimated from the rigid rotor–harmonic oscillator approximation. Vibration frequencies are scaled by 0.89. [c]ΔA $\Delta E - T\Delta S$. The positive value means that ketonand is more stable than starand.

Table 3. The difference of the thermodynamic functions between |1$_n$|ketonand and |1$_n$|starand from MM/FEP method (|1$_n$|ketonand → |1$_n$|starand) (unit: kcal/mol)

Ring Size (n, |1$_n$|)	ΔE(MM)[a]	ΔA(FEP)[b]	$-T\Delta S$[c]	ΔA(corrected)[d]
4	15.2	14.9	−0.3	76.5
5	−17.2	−22.7	−5.5	80.0
6	−133.5	−135.4	−1.9	−25.8
7	131.8	121.6	10.2	5.5

[a]The energy difference from MM calculations with the CVFF force field. [b]The free energy difference from FEP simulations with the CVFF force field. [c]The contribution of entropy: $-T\Delta S$ ΔA(FEP) – ΔE(MM). [d]The corrected free energy difference: ΔA(corrected) ΔE(MNDO) – $T\Delta S$. The positive value means that ketonand is more stable than starand.

The energy difference ΔE and the free energy difference ΔA calculated from the MM and FEP are listed in Table 3. The contribution of entropy $-T\Delta S$ was estimated from the difference between ΔE and ΔA, and also listed in the same Table. The trend of the relative stability is the same as that from MNDO calculations. Entropy has a negligible effect on the isomerism in the cases of small ring (n = 4–6). However, the contribution of the entropy to the isomerism is significant for larger |1$_7$|ketonand **4** and |1$_7$|starand **8**. For them, the entropy change plays an important role to explain the formation of **8** instead of **4**. Including the entropy effect gives the result consistent with the experiment.

The optimized structures are shown in Figures 2 and 3 to elucidate why |1$_4$|starand **5** is less stable than |1$_4$|ketonand **1**. The distances between the oxygen atoms were calculated to be around 2.3 Å for starand **5**, which are much shorter than the sum of van der Waals radii of two oxygen atoms, 3.0 Å (see the CPK representation in Figure 2). For ketonand **1**, the oxygen–oxygen distances were calculated to be 3.2–4.6 Å. Moreover, the calculation shows that each oxygen atom of **5** carries a slightly more negative charge of −0.34 |e| than −0.27 |e| of **1**. Thus, there is a larger electrostatic and steric repulsion between the oxygen atoms in **5** than in **1**, and this explains in part why **5** is less stable than **1**. Another source of the instability of **5** is strain energy involved in the

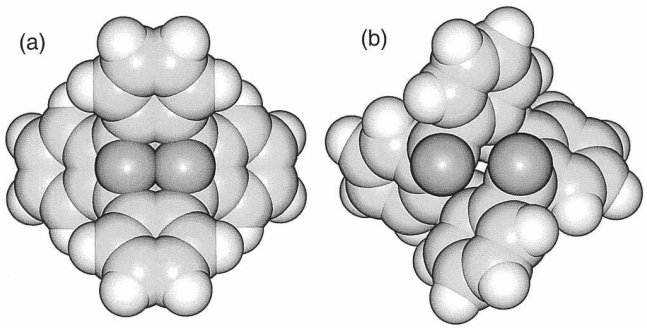

Figure 2. MNDO-optimized structures of (a) [1$_4$]starand **5** and (b) [1$_4$]ketonand **1**. The distance between the oxygen atoms are about 2.3 Å for **5** and 3.2–4.6 Å for **1**.

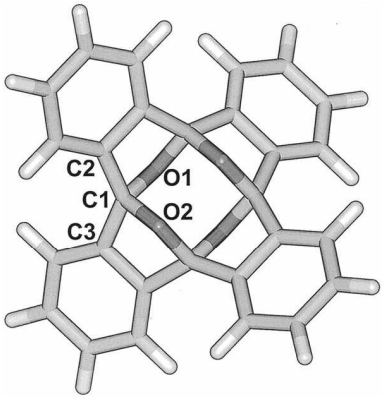

	Bond angle (in degree)
C2-C1-C3	138.7
C2-C1-O1	96.4
C2-C1-O2	107.2
O1-C1-O2	109.4

Figure 3. Bonding configurations around a carbon atom consisting the central cavity of [1$_1$]starand **5**. The bond angles around the carbon atom range from 96.4° to 138.7°.

distortion needed to reduce the electrostatic and steric repulsion between the oxygen atoms. From Figure 3, we can see that the bond angles around the carbon atoms consisting the central cavity (C_4O_4) range from 96.4° to 138.7°, far from 109.5° of the ordinary sp^3 carbon. The same arguments can be applied to the case of [1$_5$]ketonand **2** and [1$_5$]starand **6**. However, the contribution of the steric and electrostatic repulsion between oxygen atoms decreases as the ring size and the distances between the oxygen atoms increase. The small energy difference between [1$_7$]ketonand **4** and [1$_7$]starand **8**, and the large ring size of them suggest that the entropy term may affect the equilibrium between them.

Summary

The isomerism between [1$_n$]ketonand and [1$_n$]starand (n = 4–7) was investigated by the use of the semi-empirical MNDO calculation and the FEP simulation method. The calculated results are in good agreement to the experimental findings and the previously reported theoretical work. The stability of the isomers is rationalized by considering the electrostatic and steric repulsion between the oxygen atoms and the stain energy imposed on the ring to reduce the repulsion between the oxygen atoms. The large ring size of [1$_7$] makes the energy difference between two isomers less significant, and thus the energy difference between them is much smaller than any other cases. In this case, the contribution of the entropy is crucial to the isomerism.

Acknowledgment. This work has been supported by a grant from Korea Science and Engineering Foundation (Grant No. 96-0501-08-01-3), and by Ministry of Education (Grant No. BSRI-97-7402). S. H. gratefully acknowledges a postdoctoral research fellowship of Korea Research Foundation.

References

1. Glendening, E. D.; Feller, D. *J. Am. Chem. Soc.* **1996**, *118*, 6052-6059.
2. Lee, W. Y.; Park, C. H.; Kim, Y. D. *J. Org. Chem.* **1992**, *57*, 4074-4079.
3. Lee, W. Y.; Park, C. H.; Kim, S. *J. Am. Chem. Soc.* **1993**, *115*, 1184-1185.
4. Lee, W. Y.; Park, C. H. *J. Org. Chem.* **1993**, *58*, 7149-7157.
5. Lee, W. Y. *Synlett* **1994**, 765-776.
6. Lee, W. Y.; Park, C. H.; Kim, H.-J.; Kim, S. *J. Org. Chem.* **1994**, *59*, 878-884.
7. Lee, W. Y.; Park, C. H.; Kim, E. H. *J. Org. Chem.* **1994**, *59*, 4495-4500.
8. Hwang, S.; Ryu, G. H.; Lee, K. H.; Hong, J.-I.; Chung, D. S. *Bull. Korean Chem. Soc.* **1998**, *19*, 406-408.
9. Cho, S. J.; Hwang, H. S.; Park, J. M.; Oh, K. S.; Kim, K. S. *J. Am. Chem. Soc.* **1996**, *118*, 485-486.
10. Dewar, M. J. S.; Thiel, W. *J. Am. Chem. Soc.* **1977**, *99*, 4899-4907.
11. Dupius, M.; Spangler, D.; Wendoloski, J. J. *NRCC Software Catalog, Vol. 1, Program No. QG01 (GAMESS)*; University of California, Berkeley: Berkeley, CA, 1980.
12. Baker, J. *J. Comput. Chem.* **1986**, *7*, 385-395.
13. van Gunsteren, W. F. *Protein Eng.* **1988**, *2*, 5-13.
14. Mezei, M. *J. Chem. Phys.* **1987**, *86*, 7084-7088.
15. Wunz, T. P. *J. Comput. Chem.* **1992**, *13*, 667-673.
16. Orozco, M.; Luque, F. J. *J. Am. Chem. Soc.* **1995**, *117*, 1378-1386.
17. *Discover User Guide, version 95.0*; Biosym Technologies: San Diego, 1995.